JADE Note 145
July 31, 2002

Measurement of the $\ln(1/x)$ distribution using e^+e^- data at $\sqrt{s} = 22$, 35 and 44 GeV from the JADE experiment

M. Blumenstengel[(1)], O. Biebel[(1,a)] and the JADE Collaboration[(2)]

Abstract

We investigate the fragmentation function of charged particles in e^+e^- annihilation at 22, 35, and 44 GeV in terms of $\xi = \ln(1/x)$ where $x \equiv 2p/\sqrt{s}$ is the scaled momentum of a particle. Fitting a skewed gaussian function according to the parametrization of C.P. Fong and B.R. Webber the mean value $\langle\xi\rangle$, the effective QCD parameter Λ_{eff}, and the position of the maximum of the ξ distributions are determined.

(1) Max-Planck-Institut für Physik, Föhringer Ring 6, D-80805 München, Germany
contact e-mail: Otmar.Biebel@Physik.Uni-Muenchen.de
(2) for a full list of members of the JADE Collaboration see Reference [1]
(a) now at Ludwig-Maximilians-Universität München, Am Coulombwall 1, 85748 Garching, Germany

1 Introduction

The investigation of the energy dependence of momentum spectra of charged particles in hadronic final states of e^+e^- annihilation provides a significant test of QCD. In particular the combination of data taken by the experiments at the PETRA collider with those recorded up to the highest energies of LEP constitutes a large lever arm for such QCD tests. Even though the shape of the momentum spectra cannot be calculated for the complete phase space, sound predictions have been made for the shape and the energy evolution of the $\xi \equiv \ln(\sqrt{s}/2p)$ distribution [2,3], where p is the particle momentum and $\sqrt{s}$ the centre-of-mass energy.

Destructive interference for soft gluon emission suppresses the production of particles with very low momentum thus turning the ξ distribution into an approximate gaussian shape at asymptotic energies [2]. The peak position, ξ_0, of this distribution is expected to depend in leading order linearly on

$$Y \equiv \ln(\sqrt{s}/2\Lambda_{\rm eff}). \tag{1}$$

Here $\Lambda_{\rm eff}$ is related to the Λ parameter of the running strong coupling constant but not identical to it due to the approximations made in the calculation. C.P. Fong and B.R. Webber [3, 4] determined $\mathcal{O}(\alpha_S)$ corrections to the asymptotic prediction yielding a skewed gaussian shape for the ξ distribution next to its maximum:[1]

$$F_q(\xi, Y) = \frac{N(Y)}{\sigma\sqrt{2\pi}} \cdot \exp\left(\frac{k}{8} - \frac{s\delta}{2} - \frac{(2+k)\delta^2}{4} + \frac{s\delta^3}{6} + \frac{k\delta^4}{24}\right), \tag{2}$$

where $N(Y)$ is a normalization related to the multiplicity of charged particles, $\delta \equiv (\xi - \langle\xi\rangle)/\sigma$ and [3–5]

$$\langle\xi\rangle \equiv \langle\xi(Y)\rangle = \frac{Y}{2}\left(1 + \frac{\rho}{24}\sqrt{\frac{48}{\beta Y}}\right) \cdot \left[1 - \frac{\omega}{6Y}\right] + \mathcal{O}(1), \tag{3}$$

$$\sigma \equiv \sigma(Y) = \sqrt{\frac{Y}{3}}\left(\frac{\beta Y}{48}\right)^{1/4} \cdot \left(1 - \frac{\beta}{64}\sqrt{48}\beta Y\right) \cdot \left[1 + \frac{\omega}{8Y}\right] + \mathcal{O}(Y^{-1/4}), \tag{4}$$

$$s \equiv s(Y) = -\frac{\rho}{16}\sqrt{\frac{3}{Y}}\left(\frac{48}{\beta Y}\right)^{1/4} \cdot \left[1 - \frac{3\omega}{8Y}\right] + \mathcal{O}(Y^{-5/4}), \tag{5}$$

$$k \equiv k(Y) = -\frac{27}{5Y}\left(\sqrt{\frac{\beta Y}{48}} - \frac{\beta}{24}\right) \cdot \left[1 - \frac{\omega}{12Y}\right] + \mathcal{O}(Y^{-3/2}), \tag{6}$$

$$N(Y) = K \exp\left\{\left(\sqrt{\frac{48Y}{\beta}} - \frac{2\rho-\beta}{4\beta}\ln Y\right) \cdot \left[1 + \left(\sqrt{\frac{\beta}{48Y}} + \frac{2\rho-\beta}{192Y}\ln Y\right)\ln\frac{C_F}{C_A} + \frac{\omega}{12Y}\right] + \mathcal{O}(Y^{-3/2})\right\} \tag{7}$$

with $\beta \equiv 11 - 2N_f/3$, $\rho \equiv 11 + 2N_f/27$, $\omega = 1 + N_f/27$, $C_A = 3$, $C_F = 4/3$, and N_f the number of active flavours, which is usually set to 3 since gluons predominantly split into a pair of the lightest quarks (u, d, s). In Eq. (3)-(7) the terms in square brackets account for the fact that a quark initiates the shower of particles rather than a gluon, see [4, 5].

The position of the maximum of the ξ distribution, $\xi_0 \equiv \xi_0(Y)$, is related to its mean value by the relation[1]

$$\xi_0 - \langle\xi\rangle = -\frac{1}{2}\sigma s\left(1 - \frac{1}{4}\frac{k_5}{s} + \frac{5}{6}k\right) \approx \frac{3\rho}{32C_A} \approx 0.35, \tag{8}$$

[1] For simplicity the explicit Y dependence of δ, $\langle\xi\rangle$, ξ_0, σ, s, k, and k_5 is not exhibited.

description	cut
minimum track momentum	$p > 0.1$ GeV
tracks coming out of a cylinder (Ø 3 cm ×7 cm) around the e^+e^- vertex	$n_{\rm ch}^{\rm vertex} \geq 4$
tracks having $\geq$ 24 points and $p_t > 500$ MeV	$n_{\rm ch} \geq 3$
visible energy	$E_{\rm vis} = \sum_i E_i > \sqrt{s}/2$
longitudinal momentum balance	$p_{\rm bal} = \lvert \sum p_i^z / E_{\rm vis} \rvert < 0.4$
axial vertex position	$\lvert z_{\rm VTX} \rvert < 150$ mm
polar angle of thrust axis	$\lvert \cos\theta_T \rvert < 0.8$
total missing momentum	$p_{\rm miss} = \lvert \sum \vec{p}_i \rvert < 0.3 \cdot \sqrt{s}$

Table 1: Main criteria for selecting multihadronic events. E_i and $\vec{p}_i$ are energy and 3-momentum of tracks and clusters.

where the approximation is for large Y, and the numerical value is for $N_f = 5$. The function k_5 stems from a higher order correction (the fifth cumulant) to Eq. (2) [3, 5]

$$k_5 \equiv k_5(Y) = \frac{9\rho}{16}\left(\frac{3}{Y}\right)^{3/2} \cdot \left(\frac{\beta Y}{48}\right)^{1/4} + \mathcal{O}(Y^{-7/4}). \tag{9}$$

The analysis of JADE data at 22 through 44 GeV presented in this note complements the scarce data on the ξ distribution, $F_{\rm ch}(\xi, Y) \equiv 1/\sigma_{\rm tot} \cdot {\rm d}\sigma_{\rm ch}/d\xi$, available for PETRA's energy range [6], where $\sigma_{\rm tot}$ is the total cross section for non-radiative hadronic e^+e^- annihilation events, and $\sigma_{\rm ch}$ is the charged particle cross section in these events. We compare the measured ξ distributions to the Fong-Webber prediction [3], Eq. (2), and determine the free parameters of the theory, *i.e.* $N(Y)$, $\Lambda_{\rm eff}$, and one of $\langle\xi\rangle$, $\mathcal{O}(1)$, or the position of the maximum ξ_0, from a fit.

2 Detector and data samples

The study of the momentum spectra in terms of $\xi \equiv \ln(\sqrt{s}/2p)$ constitutes a re-analysis of data recorded by the JADE detector at the PETRA electron-positron collider. A detailed description of the JADE detector is given in [1, 7]. This investigation relies mainly on the central tracking detector, the jet chamber, of the JADE detector and its capability to measure precisely the tracks of charged particles and their momenta from the curvature of the tracks inside the solenoidal magnetic field of $B \approx 0.45$ T. The typical resolution of the momentum measurement is about 4.5% for a particles momentum of 1 GeV/c in the r-φ plane.[2]

For the measurement of the ξ distribution, data recorded between 1979 and 1986 at centre-of-mass energies of $\sqrt{s} = 22$, 35 and 44 GeV are analyzed. Our investigation follows the same lines as the measurement of the longitudinal and transverse cross-sections published in [8].

[2] JADE used a cylinder coordinate system with the z axis along the beam direction, the radius r is the distance from the z axis, the azimuthal angle φ is measured from the horizontal plane, and the polar angle θ is measured with respect to the z axis.

year	$\sqrt{s}$ [GeV]	data	MC
1981	22	1419	58 273
1982	34-36	14 347	171 584
1986	34-36	20 925	193 380
1984/85	43-45	4397	111 956

Table 2: Number of selected multihadronic events in data and Monte Carlo detector simulation.

The selection criteria are based on the measured tracks of charged particles in the tracking detector and on the clusters of energy deposited by the particles in the leadglass electromagnetic calorimeter. Applying the criteria listed in Tab. 1 to the multihadronic events which are selected as described in [9] yielded the number of events in data and Monte Carlo simulation (MC) listed in Tab. 2. We do not include the data taken at $\sqrt{s} \approx 14$ GeV since detailed simulation studies showed that the ξ distribution is strongly affected by the electroweak decays of B hadrons which would introduce a significant dependence of the ξ distribution on the modeling of these decays.

Contrary to our previous publications [8,9] we use MC simulation data based on the PYTHIA 5.722 event generator [10] tuned to the high statistics LEP data by the OPAL collaboration [11]. These data have been generated using the original JADE simulation software adapted to run on modern computers [12]. Detailed investigations [12] revealed an excellent description of the JADE data by the tuned PYTHIA generator run at the centre-of-mass energies considered for this analysis. None of the parameters controlling the quality of the detector simulation have been changed compared with their original values. Thus, as in our measurement of the longitudinal and transverse cross-section [8], we adapt the simulated data to the experimental position of the e^+e^- collision point (I.P.) and to apply appropriate gaussian smearing on the simulated z vertex position, z_{VTX}, and on the minium radial distance of a track to the I.P., d_0.

The two data sets taken around 35 GeV are corrected separately for detector acceptance and efficiencies since the corresponding detector layouts changed between these two periods of data taking. The two ξ distributions will be combined, however, after the corrections for detector effects are applied.

3 Measurement of the ξ distribution at JADE

All charged particles whose tracks comply with the selection criteria listed in Tab. 1 are used in the measurement of the ξ distribution. The width of the bins in ξ are chosen such that bin migration effects due to the finite momentum resolution are negligible. This allows to apply a bin-by-bin correction method to correct for the effects of limited detector acceptance and resolution.

The comparison of the measured ξ distribution with the results from the Monte Carlo (MC) simulation shows small deviations of the order of -3.3% to $+1.4\%$ of the total multiplicity, *i.e.* the integral of the ξ distribution. Such small deviations might be expected since we use the PYTHIA event generator at $\sqrt{s} = 22$, 35, and 44 GeV which was tuned to describe OPAL data recorded at $\sqrt{s} = 91$ GeV [11]. We account for the differences by scaling the MC distributions by a global factor individually for each data taking period ($n_{\mathrm{cor}} = 0.9897$, 1.0044, 0.9672, 1.0138 for the data taken at 22, 35 (1982), 35 (1986), 44 GeV, respectively). The multiplicative correction factors for any detector effects are determined from the PYTHIA MC simulation.

Fig. 1 shows the ξ distribution measured from the four data sets and corrected for the limited acceptance and resolution of the detector and for initial state radiation (ISR). The error bars exhibit the statistical uncertainties only. The simulated ξ distribution with the global scaling

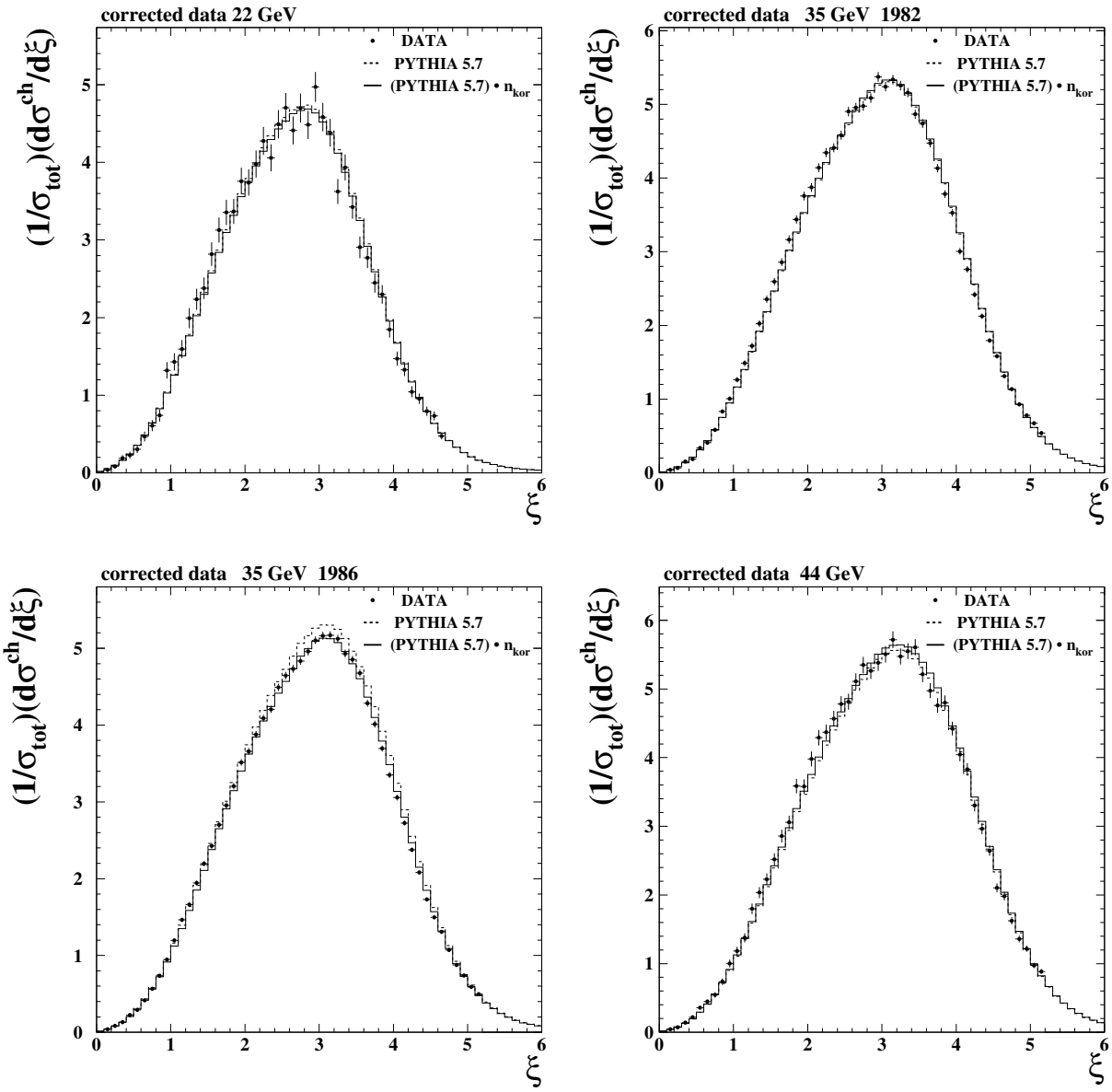

Figure 1: Measured ξ distributions corrected for detector effects. The results from the simulation before and after application of the global multiplicity scaling factor are superimposed in each case.

factor applied is superimposed on the data points in Fig. 1. The agreement between data and simulation is acceptable.

The detector correction applied to the measured ξ distributions are shown in Fig. 2. Around the position of the maximum in the ξ distribution the correction is less than 10% while it increases up to +35% and down to −50% towards the kinematic limits of the distribution. These significant corrections at large ξ are due to additional particles from interactions in the detector material, *e.g.* photon conversion.

From the corrected ξ distributions shown in Fig. 1 the position of the maximum is determined by fitting Eq. (2). Before fitting the two corrected ξ distributions obtained from the data taken

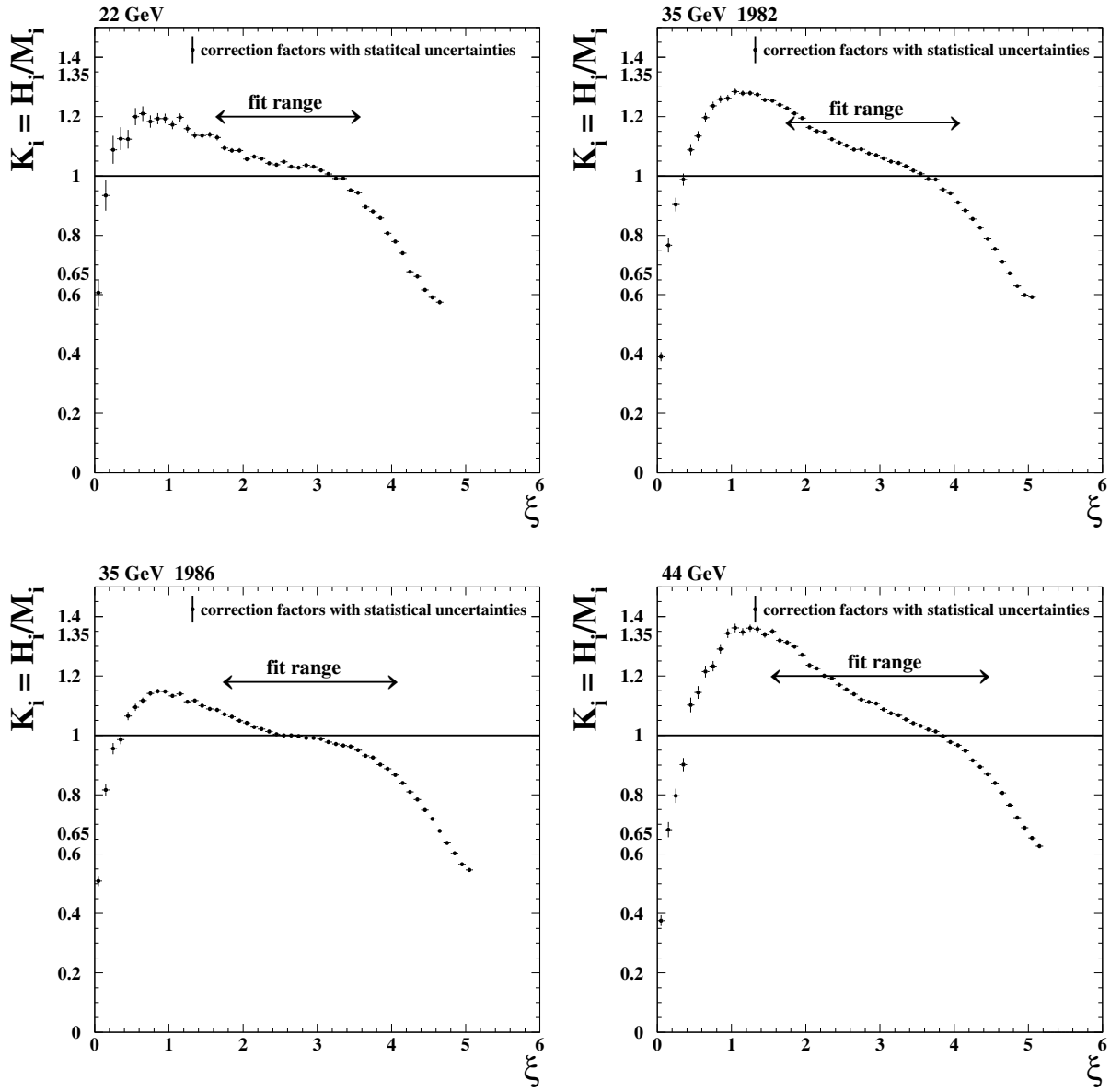

Figure 2: Factors K_i to correct for finite detector resolution and acceptance and initial state radiation (ISR). H_i corresponds to the ξ distribution generated by PYTHIA without ISR while M_i is the ξ distribution found when the fully simulated data including ISR undergo the same selection and measurement procedure as the measured data.

around 35 GeV in 1982 and 1986 have been combined. The fit considers three parameters N, Λ_{eff} (Eq. (1)), and one of $\langle\xi\rangle$, $\mathcal{O}(1)$, or the position of the maximum ξ_0. The remaining parameters of the skewed gaussian (2) are calculated using the relations (4)-(6). When fitting $\mathcal{O}(1)$ we use Eq. (3). In case of using ξ_0 the asymptotic relation (8) is employed to substitute $\langle\xi(Y)\rangle$ in Eq. (2).

As the skewed gaussian shape calculated in next-to-leading log approximation (NLLA) is applicable only close to the maximum region, the fit range has to be chosen with some care. The range of the ξ distribution considered for the fits is selected according to

22 GeV	$\Lambda_{\rm eff}$ (GeV)	N	$\langle\xi\rangle$	$\mathcal{O}(1)$	ξ_0
Fit results	0.272	11.61	2.366	-0.99	2.735
Statistics	±0.046	±0.31	±0.020	±0.12	±0.019
Fit range ±0.1	±0.009	±0.07	±0.006	±0.02	±0.007
two Gaussian					±0.077
$\lvert\cos\theta_T\rvert < (0.7\cdots0.9)$	±0.021	±0.19	±0.009	±0.06	±0.007
$E_{\rm vis} > (0.95\cdots1.05)\sqrt{s}/2$	±0.002	±0.02	±0.002	±0.01	±0.002
$n_{\rm ch} \geq 7$	±0.009	±0.03	±0.014	±0.01	±0.014
$n_{\rm ch}^{\rm vertex} \geq 7$	±0.009	±0.03	±0.004	±0.02	±0.003
$p_{\rm bal} < (0.3\cdots\infty)$	±0.004	±0.04	±0.002	±0.06	±0.002
$p_{\rm miss} < (0.25\cdots\infty)\sqrt{s}$	±0.004	±0.04	±0.002	±0.02	±0.003
$d_0 < (9\cdots16)$ mm	±0.011	±0.13	±0.021	±0.04	±0.020
$\lvert z_{\rm VTX} - \langle z_{\rm VTX}\rangle\rvert < (24\cdots32)$ mm	±0.008	±0.07	±0.003	±0.02	±0.003
HERWIG 5.9	±0.004	±0.03	±0.072	±0.04	±0.036
JETSET 6.3	±0.006	±0.06	±0.002	±0.01	±0.003
Total syst. error	±0.030	±0.27	±0.047	±0.08	±0.090
Total error	±0.055	±0.41	±0.051	±0.14	±0.092

Table 3: Results and systematic uncertainties of the fits to the ξ distribution measured at 22 GeV.

- symmetry around the maximum,
- not exceeding the kinematic boundary $\xi_R = \ln\left(\sqrt{s}\Big/2\sqrt{p^2+Q_0^2}\right)$ [13], where p is the particle's momentum and $Q_0 \approx 2m_\pi$,
- obtaining a good description of the shape of the ξ distribution by the distorted gaussian in terms of χ^2/d.o.f. since a large χ^2/d.o.f. would indicate a range bigger than the scope of application of the skewed gaussian function,
- use of a range where detector corrections are less than about $\pm35\%$.

This resulted in the ranges 1.65-3.55, 1.75-4.05, and 1.75-4.25 for the data sets taken at 22, 35, and 44 GeV respectively. The fits using statistical errors only yielded χ^2/d.o.f. of 1.4, 2.0, 1.1 for these three data sets. The tables 3-5 list the results after performing the fit separately at each energy point. In particular it is found that the fits yield within the small statistical uncertainties the same results for $\Lambda_{\rm eff}$ and $N(Y)$ independently of which of $\langle\xi(Y)\rangle$, $\mathcal{O}(1)$, or $\xi_0(Y)$ is used as the third variable in the fit. The statistical correlation of the fit parameters for the three different sets of parameters is shown in Tab. 6.

To assess the systematic uncertainties we varied the multihadronic selection criteria listed in Tab. 1. The variations are specified in tables 3-5 together with the resulting changes of the fit parameters. In addition the stability of the fit results is checked by simultaneously enlarging and shrinking the fit range by $\Delta\xi = 0.1$. The range of variation of d_0 and $\lvert z_{\rm VTX} - \langle z_{\rm VTX}\rangle\rvert$ are determined from fitting the sum of a narrow and a broad gaussian to the distribution of d_0 and $\lvert z_{\rm VTX} - \langle z_{\rm VTX}\rangle\rvert$, respectively, and taking two and three times the width of the broader gaussian. The dependence on the particular Monte Carlo event generator used for the correction of the detector effects is investigated by using alternatively HERWIG5.9 [14] and JETSET6.3 [15]. When using ξ_0 as a fit parameter, we checked the position of the maximum by applying a different method which considers a fit of two gaussian functions with different widths for the

35 GeV	$\Lambda_{\rm eff}$ (GeV)	N	$\langle\xi\rangle$	$\mathcal{O}(1)$	ξ_0
Fit results	0.284	14.06	2.687	-0.904	3.064
Statistics	±0.008	±0.05	±0.020	±0.019	±0.003
Fit range ±0.1	±0.003	±0.02	±0.004	±0.008	±0.001
two Gaussian					±0.044
$\lvert\cos\theta_T\rvert < (0.7\cdots0.9)$	±0.003	±0.06	±0.003	±0.014	±0.002
$E_{\rm vis} > (0.95\cdots1.05)\sqrt{s}/2$	±0.004	±0.01	±0.001	±0.002	±0.001
$n_{\rm ch} \geq 7$	±0.002	±0.03	±0.001	±0.006	±0.001
$n_{\rm ch}^{\rm vertex} \geq 7$	±0.002	±0.04	±0.001	±0.003	±0.001
$p_{\rm bal} < (0.3\cdots\infty)$	±0.002	±0.01	±0.001	±0.002	±0.001
$p_{\rm miss} < (0.25\cdots\infty)\sqrt{s}$	±0.002	±0.02	±0.001	±0.002	±0.001
$d_0 < (9\cdots16)$ mm	±0.034	±0.15	±0.015	±0.020	±0.014
$\lvert z_{\rm VTX} - \langle z_{\rm VTX}\rangle\rvert < (24\cdots32)$ mm	±0.038	±0.61	±0.001	±0.004	±0.002
HERWIG 5.9	±0.004	±0.07	±0.010	±0.013	±0.010
JETSET 6.3	±0.006	±0.08	±0.001	±0.008	±0.009
Total syst. error	±0.052	±0.63	±0.019	±0.034	±0.047
Total error	±0.053	±0.64	±0.019	±0.039	±0.047

Table 4: Results and systematic uncertainties of the fits to the ξ distribution measured at 35 GeV.

44 GeV	$\Lambda_{\rm eff}$ (GeV)	N	$\langle\xi\rangle$	$\mathcal{O}(1)$	ξ_0
Fit results	0.220	16.42	2.809	-1.08	3.193
Statistics	±0.018	±0.17	±0.010	±0.06	±0.010
Fit range ±0.1	±0.017	±0.17	±0.005	±0.05	±0.019
two Gaussian					±0.004
$\lvert\cos\theta_T\rvert < (0.7\cdots0.9)$	±0.004	±0.12	±0.006	±0.02	±0.005
$E_{\rm vis} > (0.95\cdots1.05)\sqrt{s}/2$	±0.002	±0.02	±0.003	±0.01	±0.003
$n_{\rm ch} > 7$	±0.030	±0.34	±0.014	±0.06	±0.016
$n_{\rm ch}^{\rm vertex} > 7$	±0.038	±0.14	±0.024	±0.11	±0.026
$p_{\rm bal} < (0.3\cdots\infty)$	±0.002	±0.01	±0.001	±0.01	±0.002
$p_{\rm miss} < (0.25\cdots\infty)\sqrt{s}$	±0.002	±0.01	±0.003	±0.01	±0.003
$d_0 < (9\cdots16)$ mm	±0.022	±0.24	±0.015	±0.01	±0.042
$\lvert z_{\rm VTX} - \langle z_{\rm VTX}\rangle\rvert < (24\cdots32)$ mm	±0.003	±0.03	±0.005	±0.01	±0.005
HERWIG 5.9	±0.005	±0.07	±0.013	±0.03	±0.013
JETSET 6.3	±0.002	±0.14	±0.001	±0.01	±0.001
Total syst. error	±0.056	±0.59	±0.043	±0.18	±0.063
Total error	±0.059	±0.62	±0.044	±0.19	±0.064

Table 5: Results and systematic uncertainties of the fits to the ξ distribution measured at 44 GeV.

22 GeV	N	$\langle\xi\rangle$
$\Lambda_{\rm eff}$	-0.923	$+0.446$
N		-0.429

N	$\mathcal{O}(1)$
-0.902	$+0.983$
	-0.891

N	ξ_0	
-0.930	$+0.320$	$\Lambda_{\rm eff}$
	-0.316	N

35 GeV	N	$\langle\xi\rangle$
$\Lambda_{\rm eff}$	-0.890	$+0.443$
N		-0.426

N	$\mathcal{O}(1)$
-0.845	$+0.979$
	-0.835

N	ξ_0	
-0.890	$+0.336$	$\Lambda_{\rm eff}$
	-0.332	N

44 GeV	N	$\langle\xi\rangle$
$\Lambda_{\rm eff}$	-0.881	$+0.369$
N		-0.360

N	$\mathcal{O}(1)$
-0.877	$+0.983$
	-0.877

N	ξ_0	
-0.886	$+0.226$	$\Lambda_{\rm eff}$
	-0.272	N

Table 6: Statistical correlations of the fit parameters for the three different sets of parameters investigated ($\Lambda_{\rm eff}$, N, and one of $\langle\xi\rangle$, $\mathcal{O}(1)$, ξ_0). Only the non-trivial off-diagonal correlation coefficients are shown.

part to the left and to the right of the maximum but the same parameters for the normalization and central value. This is labelled "two Gaussian" in tables 3-5. It is used since the results of [17], which are used for an investigation of the energy dependence of ξ_0 in [18], were obtained using this approach.

Symmetric systematic errors are assigned for a particular variation which are calculated by taking half of the maximum difference between all the results, *i.e.* the results obtained by the standard procedure and by the varied procedure. Since the data statistics is feeble at 22 GeV we investigated whether the systematic changes of the fit results observed by varying the selection cuts, which changes the size of the data sample, are due to statistical fluctuations. We find that in general only the smaller of the systematic errors assigned are compatible with the expected statistical uncertainty. Thus the systematic errors are not dominated by statistical fluctuations.

In general, the systematic uncertainties are small. However, exceptions are the variations of the cuts on d_0, $|z_{\rm VTX} - \langle z_{\rm VTX}\rangle|$, $n_{\rm ch}$, and $n_{\rm ch}^{\rm vertex}$. These contribute significantly to the total systematic uncertainty at 35 and 44 GeV. The reason for $n_{\rm ch}$ and $n_{\rm ch}^{\rm vertex}$ is the few percent difference in the measured and simulated multiplicity of charged particles. This leads to a larger uncertainty if the cut gets closer to the average number of charged particles observed. Since these two cuts require well-reconstructed tracks they will reject events which have many low energy but very few high energy particles, this affects the position of the maxium, the mean value, the multiplicity and also the other parameters due to the correlations.

In the case of varying the cuts on d_0 and $|z_{\rm VTX} - \langle z_{\rm VTX}\rangle|$ detailed investigations showed that the deviation between data and simulation in these variables is in fact ξ dependent. Such deviations could be caused by multiple scattering due to additional material next to the interaction point in the real detector which is not simulated. Applying a ξ dependent reweighting of the simulated d_0 and $z_{\rm VTX}$ values to account for such effects due to additional multiple scattering reduced the systematic uncertainty. The remaining part is due to the tight cuts which need to be chosen to reject particles from decays and secondary interactions in the detector material which enhances the deficiencies of the Monte Carlo simulation due to the larger correction required.

In the case of the maximum position the dominating contribution to the systematic uncertainty is due to the use of the "two Gaussian" shape.

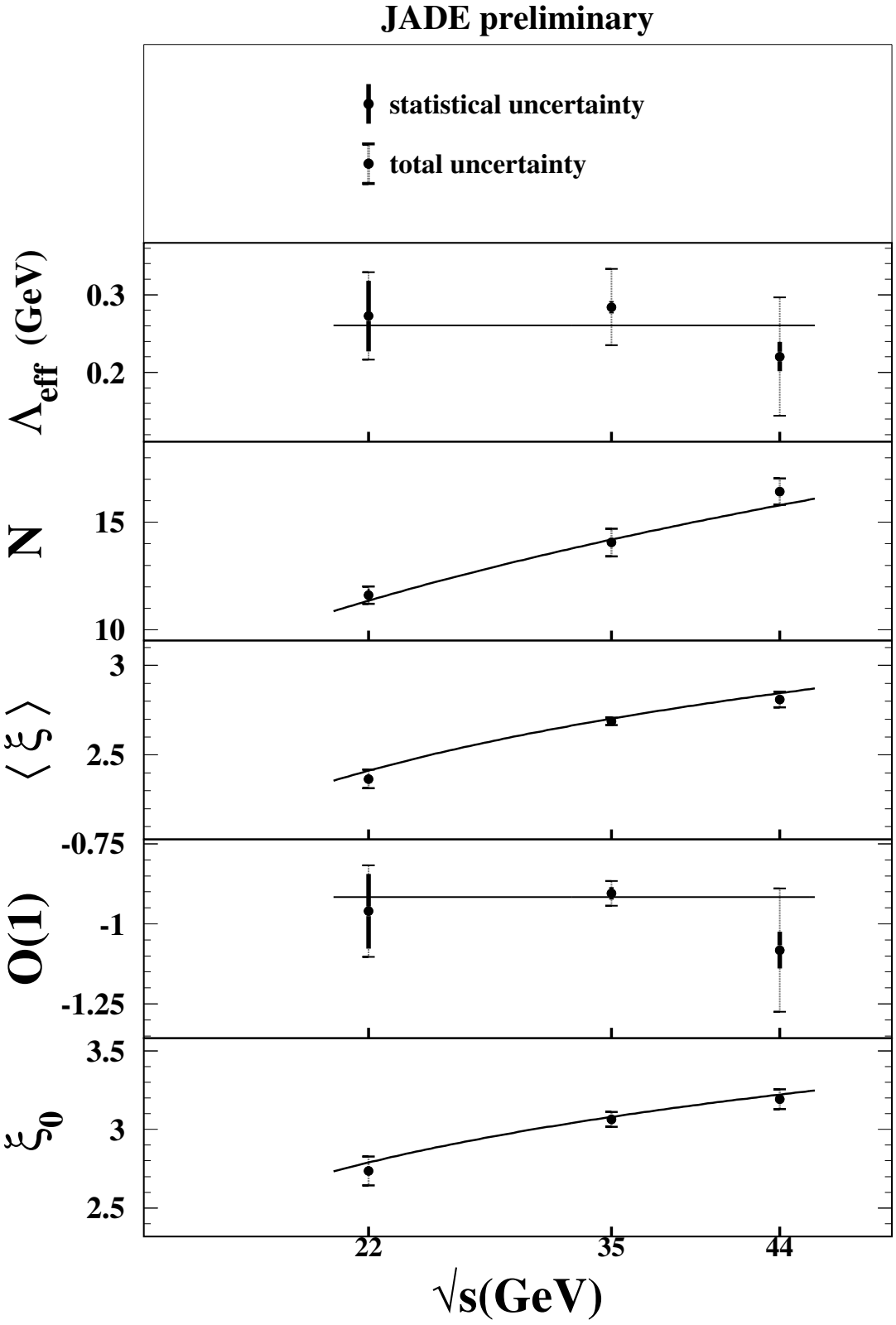

Figure 3: Results for $\Lambda_{\rm eff}$, N, $\langle\xi\rangle$, $\mathcal{O}(1)$, ξ_0 versus the centre-of-mass energy $\sqrt{s}$. The error bars indicate the statistical (thick line) and total uncertainties (thin line with horizontal tick marks). The curves are described in the text.

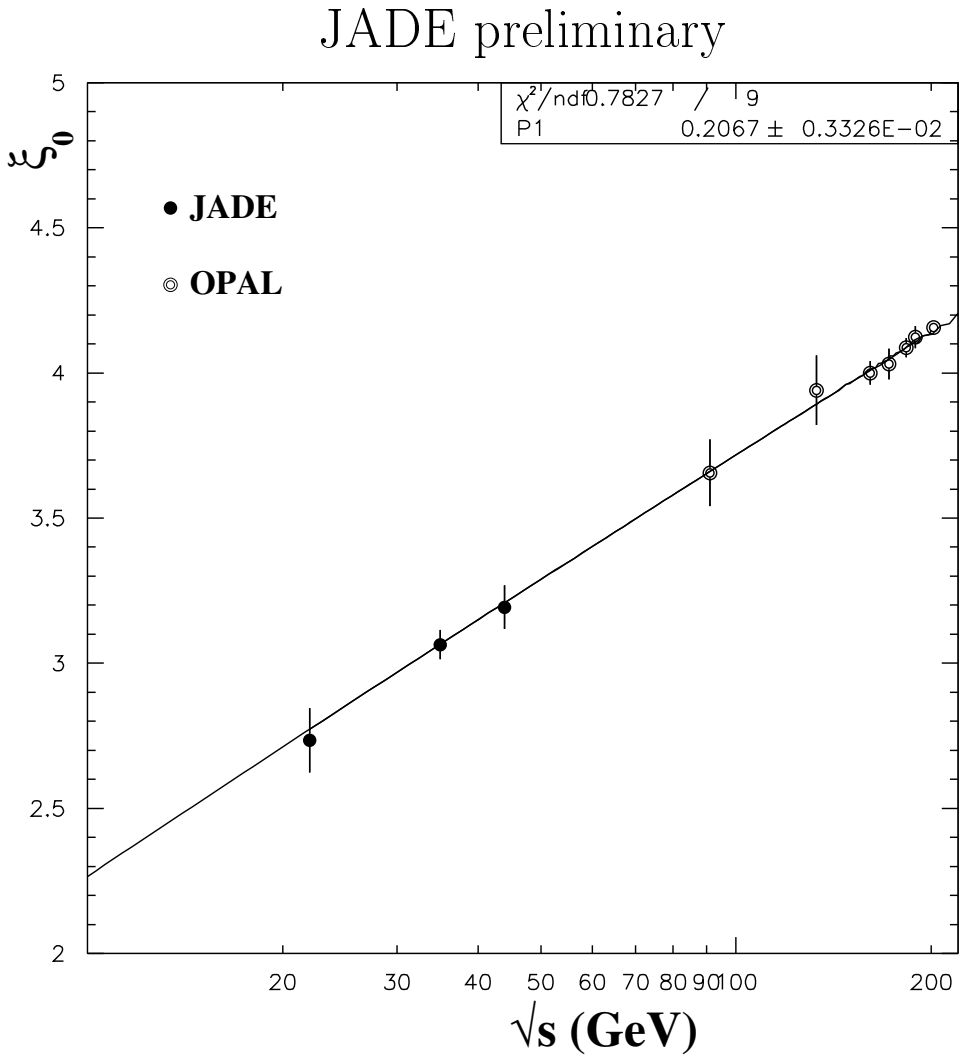

Figure 4: The measured position of the maximum ξ_0 is shown together with results at higher centre-of-mass energies. The curve is the expectation of QCD in NLLA, Eqs. (8) and (3).

4 Summary and conclusions

The final results of the fitted parameters including statistical and systematic uncertainties are summarized in Fig. 3. The results indicate $\Lambda_{\rm eff} \approx$ const., $\mathcal{O}(1) \approx$ const., and $N(Y)$, $\langle\xi(Y)\rangle$ and $\xi_0(Y)$ increase with $Y \equiv \ln(\sqrt{s}/2\Lambda_{\rm eff})$. Considering the systematic errors to be fully correlated, weighted averages can be calculated for $\Lambda_{\rm eff}$ and $\mathcal{O}(1)$ using the total errors for the weights. This yields

$$\begin{aligned} \Lambda_{\rm eff} &= (0.261 \pm 0.047)\ \text{GeV} \\ \mathcal{O}(1) &= -0.916 \pm 0.047 \end{aligned}$$

where total errors are quoted. These values are indicated in Fig. 3 by a horizontal line. The average value for $\Lambda_{\rm eff}$ is in agreement with the results found in several studies of the ξ distribution at higher centre-of-mass energies (*e.g.* [17]).

In Fig. 3 also the curves from the NLLA calculations Eqs. (3) and (8) are overlaid using the average values of $\Lambda_{\rm eff}$ and $\mathcal{O}(1)$ given above. For $N(Y)$ Eq. (7) is shown in the figure. The

unknown constant of proportionality, K, which relates $N(Y)$ to the exponential term in Eq. (7) has been fitted for the curve shown in Fig. 3. In all cases the NLLA formulae (3), (7) and (8) agree well with the data.

More detailed tests require to consider measurements of these quantities over a larger range of centre-of-mass energies, *e.g.* [17] as is shown in Fig. 4. Since the flavour composition changes with energy due to the different couplings of the intermediate photon and Z boson to the quarks, such a study should allow to test possible flavour dependent effects due to finite quark masses, in particular on the position of the maximum ξ_0 [18].

References

[1] B. Naroska, Phys. Rep. **148** (1987) 67.

[2] Yu.L. Dokshitzer, V.S. Fadin, and V.A. Khoze, Phys. Lett. **B115** (1982) 242.

[3] C.P. Fong and B.R. Webber, Nucl. Phys. **B355** (1991) 54.

[4] C.P. Fong and B.R. Webber, Phys. Lett. **B241** (1990) 255.

[5] Yu.L. Dokshitzer, V.A. Khoze, C.P. Fong, and B.R. Webber, Phys. Lett. **B273** (1991) 319.

[6] TASSO Collab., W. Braunschweig et al., Z. Phys. **C47** (1990) 187.

[7] JADE Collab., W. Bartel et al., Phys. Lett. **88B** (1979) 171;
JADE Collab., W. Bartel et al., Phys. Lett. **129B** (1983) 145.

[8] M. Blumenstengel, O. Biebel, P.A. Movilla Fernández, P. Pfeifenschneider, S. Bethke, S. Kluth and the JADE Collab., Phys. Lett. **B571** (2001) 37.

[9] P.A. Movilla Fernández, O. Biebel, S. Bethke, S. Kluth, P. Pfeifenschneider and the JADE Collab., Eur. Phys. J. **C1** (1998) 461.

[10] T. Sjöstrand, *PYTHIA 5.7 and JETSET 7.4 Physics and Manual*, CERN-TH-7112-93;
T. Sjöstrand: Comput. Phys. Commun. **82** (1994) 74.

[11] OPAL Collab., G. Alexander et al.: Z. Phys. **C69** (1996) 543.

[12] P.A. Movilla Fernández: *Determinations of* α_S *at* $\sqrt{s} = 14$ *to* 44 *GeV using Resummed Calculations*, JADE Note 144, March 15, 2002 (unpublished).

[13] W. Ochs, private communication.

[14] G. Marchesini et al.: Comput. Phys. Commun. **67** (1992) 465;
We used the tune of Ref. [11] for this generator.

[15] T. Sjöstrand: Comput. Phys. Commun. **39** (1986) 347;
T. Sjöstrand and M. Bengtsson: Comput. Phys. Commun. **43** (1987) 367;
We used the tune obtained by the JADE collaboration [16], see Ref. [12].

[16] JADE Collab., E. Elsen et al., Z. Phys. **C46** (1990) 349.

[17] OPAL Collab., M.Z. Akrawy et al., Phys. Lett. **B247** (1990) 617; OPAL Collab., G. Alexander et al., Z. Phys. **C72** (1996) 191; OPAL Collab., K. Ackerstaff et al., Z. Phys. **C75** (1997) 193; OPAL Collab., G. Abbiendi et al., Eur. Phys. J. **C16** (2000) 185.

[18] M. Blumenstengel et al., in progress.